



# Insights into the age of the Mono Lake Excursion and magmatic crystal residence time from (U-Th)/He and $^{230}\text{Th}$ dating of volcanic allanite

Stephen E. Cox <sup>a,\*</sup>, Kenneth A. Farley <sup>a</sup>, Sidney R. Hemming <sup>b</sup>

<sup>a</sup> Division of Geological and Planetary Sciences, California Institute of Technology, Pasadena, CA 91125, USA

<sup>b</sup> Department of Earth and Environmental Sciences and Lamont-Doherty Earth Observatory of Columbia University, Palisades, NY 10964, USA

## ARTICLE INFO

### Article history:

Received 31 August 2011

Received in revised form 13 December 2011

Accepted 15 December 2011

Available online xxx

Editor: B. Marty

### Keywords:

allanite

Mono Lake Excursion

Laschamp Excursion

(U-Th)/He

residence time

Wilson Creek

## ABSTRACT

We present new data for the age of the Mono Lake Excursion at its type locality. Using the (U-Th)/He system on allanite, we dated Wilson Creek Ash 15 (Lajoie, 1968) to  $38.7 \pm 1.2$  ka (2 SE). The new age for this ash supports the hypothesis (Kent et al., 2002; Zimmerman et al., 2006) that the Mono Lake Excursion is coincident with, and probably the same event as, the Laschamp Geomagnetic Excursion ( $40.4 \pm 2$  ka), an event that shares similar magnetic characteristics with the excursion identified at Mono Lake. We also estimate an allanite magma residence time of slightly less than 30 ka based on  $^{230}\text{Th}/^{238}\text{U}$  disequilibrium and the (U-Th)/He-based eruption age.

© 2011 Elsevier B.V. All rights reserved.

## 1. Introduction

Mono Lake is a closed-basin lake in the western Great Basin, east of the Sierra Nevada in California. The ancient lake sediments of the Mono Basin contain important regional climate records (Benson et al., 1990, 1997, 1998; Bursik and Gillespie, 1993; Davis, 1999; Graham and Hughes, 2007; Lajoie, 1968; Reheis et al., 2002; Russell, 1889; Stine, 1987, 1990a, 1990b; Zimmerman et al., 2006, 2011a, 2011b) that can be dated in a relative sense by correlation of the volcanic ashes that occur throughout the basin. The Upper Pleistocene Wilson Creek Formation (WCF), first mapped by Lajoie (1968), comprises unconsolidated lake sediments punctuated by eighteen rhyolitic ashes and one basaltic ash that have been numbered and bundled into marker sequences. These ashes can be identified with confidence simply based upon outcrop appearance and stratigraphic order.

While these ashes provide closely spaced relative age constraints for climate records from the last glacial period in the Mono Basin, absolute ages are difficult to obtain due to the youth of the ashes and geochemical complications in Mono Lake. Low in situ produced daughter product concentrations and uncertainty about initial compositions and secular equilibrium pose challenges for most radiometric dating systems in

such juvenile materials. While  $^{14}\text{C}$  dating is frequently used for materials younger than ~50 ka, several unique problems such as a large and almost certainly time-varying dead carbon reservoir and extreme carbonate chemistry plague radiocarbon dating attempts in this hypersaline alkaline lake (Benson et al., 1990; Cassata et al., 2010; Kent et al., 2002; Zimmerman et al., 2006).  $^{40}\text{Ar}/^{39}\text{Ar}$  dating of several WCF ashes suffers from significant variability due to inheritance and high uncertainties in the results (Cassata et al., 2010; Chen et al., 1996; Kent et al., 2002; Zimmerman et al., 2006). In this work, we present new (U-Th)/He eruption age data for allanites from the ash associated with the prominent magnetic excursion known as the Mono Lake Excursion (Liddicoat and Coe, 1979; Lund et al., 1988) at its type locality and also present U-Th disequilibrium data that bears on the allanite crystal residence time in the magma chamber.

## 2. Geologic background

### 2.1. The age of Ash 15 in the Wilson Creek Formation

One of the most intriguing WCF ashes is Ash 15 (Lajoie, 1968), which bisects a geomagnetic excursion first identified by Denham and Cox (1971), who were in search of expressions of the Laschamp Excursion. Because the excursion appeared to lack the negative inclinations characteristic of the Laschamp Excursion, and because existing age estimates led them to think this excursion was too old to be

\* Corresponding author.

E-mail address: [scox@caltech.edu](mailto:scox@caltech.edu) (S.E. Cox).

the Laschamp, Denham and Cox (1971) concluded that the Laschamp Excursion was not present in the section, and that they had identified a previously unknown excursion. Liddicoat and Coe (1979) better characterized this event and named it the Mono Lake Excursion.

In the following decades, the age of the Laschamp Excursion was refined to  $40.4 \pm 2$  ka (Guillou et al., 2004). Many authors now believe that the Mono Lake Excursion must be younger than this, at  $\sim 32$ – $34$  ka, based on a carbonate radiocarbon timescale and correlation to a contemporaneous geomagnetic excursion present in some marine records (Benson et al., 1998, 2003; Cassata et al., 2010; Laj et al., 2004).

New dating efforts have substantially revised the timescale of the Wilson Creek Formation (Benson et al., 1998, 2003; Cassata et al., 2010; Kent et al., 2002; Zimmerman et al., 2006). Carbonate U–Th disequilibrium dating of cross cutting calcite indicates that the formation extends to at least 49 ka (Xianfeng Wang, unpublished  $^{238}\text{U}$ – $^{230}\text{Th}$  measurement, personal communication), and it almost certainly extends to greater than 60 ka (Cassata et al., 2010; Kent et al., 2002; Zimmerman et al., 2006). It is clear that the two geomagnetic excursions observed between 30 and 45 ka in some marine records (Laj et al., 2004) fall within the time span of the apparently continuous high-resolution sediment record at Mono Lake.

Liddicoat and Coe (1979) demonstrated the presence of negative inclinations in the event at Mono Lake, casting doubt on the original evidence that precluded the event in Mono Lake from being the Laschamp. One possibility is that the Mono Lake Excursion is in fact the Laschamp Excursion, as suggested by Kent et al. based on the constraints that radiocarbon ages represent minimum depositional ages and that the  $^{40}\text{Ar}/^{39}\text{Ar}$  sanidine ages represent maximum depositional ages (Kent et al., 2002).

Zimmerman et al. (2006) created a timescale for the WCF based on a correlation of the paleomagnetic record in the sediments to the GLOPIS stack (Laj et al., 2004). In this timescale, Ash 15 falls at 39.8 ka, overlapping the Laschamp Excursion at its type locality. Ash 15 is about 20 cm above the paleointensity low in the Mono Lake record, which has an average sedimentation rate of  $\sim 20$  cm/ka (Zimmerman et al., 2006). Models that place the excursion preserved in the Mono Lake sediments near 34 ka and fit the Laschamp to another feature in the paleointensity record either directly violate concordant radiocarbon and  $^{40}\text{Ar}/^{39}\text{Ar}$  ages higher in the core, imply large fluctuations in sedimentation rates that are not correlated with any known tectonic, volcanic, or climatic events (Zimmerman et al., 2006), or produce significant mismatch of the paleointensity patterns at the key interval of interest (Cassata et al., 2010). Attempts to constrain the entirety of the Wilson Creek Formation to the time period after the Laschamp (e.g., Model B in Cassata et al., 2010) are unable to produce a feasible paleomagnetic correlation and imply even larger fluctuations in sedimentation rate. Cassata et al. (2010) force the paleomagnetic intensity minimum in the Mono Lake record to correspond to a 34 ka minimum in the GLOPIS record and argue that the low sedimentation rates implied before 34 ka would not have captured the Laschamp. However this line of reasoning demands independent evidence for such a sedimentation rate change, which is currently lacking.

Even when excursions and reversals are well expressed globally, single paleomagnetic records are fragmented due to inconsistent sedimentation and may not preserve such short duration events (Coe et al., 2004). The difficulty of resolving short events in a single paleomagnetic record and the uncertainties in correlation pointed out by Cassata et al. (2010) demand a direct date for the excursion.

## 2.2. (U–Th)/He dating of juvenile materials

Dating of young volcanic samples using the (U–Th)/He system can be undertaken on uranium- and thorium-rich minerals that quantitatively retain helium, such as zircon, monazite, xenotime,

sphene, allanite, and garnet. For example, Aciego et al. (2003) dated garnets from the 79 AD eruption of Mount Vesuvius, and Farley et al. (2002) dated apatite and zircon from the 330 ka Rangitawa tephra. Davidson et al. (2004) demonstrated the application of the (U–Th)/He chronometer to young volcanic rocks that cannot be easily dated using the  $^{40}\text{Ar}/^{39}\text{Ar}$  technique. Application of this method to samples with such young crystallization ages requires potentially uncertain uranium–thorium disequilibrium corrections that must be measured or modeled. Thus in many cases the precision of the radiocarbon and  $^{40}\text{Ar}/^{39}\text{Ar}$  systems is superior. However, lack of appropriate material, contamination, inheritance, and other problems sometimes favor use of the (U–Th)/He technique. Ash 15, which cannot be reliably dated using more established techniques (Cassata et al., 2010; Zimmerman et al., 2006), is one such case.

Allanite ((Ca,REE) $_2$ Al $_2$ Fe $_2$ Si $_3$ O $_{12}$ OH) is an epidote group mineral common in Ash 15. It typically carries high concentrations of thorium, in this case up to 1 wt.% (Table 1), making it an appealing choice for dating of very young samples. Previous (U–Th)/He dating of allanite is very limited: Wolf (1997) dated a sample from the Peninsular Ranges batholith and concluded this phase has a He closure temperature  $> 100$  °C. Ash 15 is an unwelded tephra deposit, indicating that pumice lapilli cooled to very low temperatures during ascent and fall, a geologically instantaneous event. The deposit was never deeply buried or heated, so the observation of Wolf (1997) is sufficient to ensure quantitative retention of He in the allanite beginning immediately after eruption and deposition.

## 2.3. Magmatic crystal residence time from $^{238}\text{U}$ – $^{230}\text{Th}$ disequilibrium

Disequilibrium in the actinide decay chains at the time of eruption violates the assumption of secular equilibrium that underlies standard helium dating, and can lead to erroneous ages in young samples due to the different decay rates of different isotopes of U and Th (Farley et al., 2002). Isotopic disequilibrium must therefore be measured in order to date young samples. Because U and Th are retained after crystallization in minerals such as allanite (Vazquez and Reid, 2004) and zircon (e.g., Crowley et al., 2007; Schmitt et al., 2003), this disequilibrium can also be used as a crystallization chronometer. The ratio of the current excess of a given isotope that is out of equilibrium ( $^{230}\text{Th}$  in this study) to the initial excess at the time of crystallization, which can be inferred based on the observed partitioning of more stable isotopes of the same element, is a function of the time since crystallization. In conjunction with an eruption chronometer such as a (U–Th)/He age, this allows the calculation of a residence time in the magma for the crystal.

## 3. (U–Th)/He and $^{230}\text{Th}$ dating methods

### 3.1. Sampling and allanite separation

We collected Ash 15 at the South Shore outcrop ( $37^{\circ}59'11''\text{N}$ ,  $118^{\circ}54'44''\text{W}$ ) on the southeast shore of modern Mono Lake. After removing the  $\sim 50$  cm weathered layer of the outcrop, we removed clean samples of the ash with a spackling knife. We took the sample from the uppermost coarse layer of the 24 cm unconsolidated ash bed, which has distinctive layering (See Supplementary Fig. 1). We washed the sample in a  $63\ \mu\text{m}$  sieve and processed the coarse fraction first through lithium heteropolytungstate ( $\rho = 2.85$ ) and then methylene iodide ( $\rho = 3.32$ ). We then removed ferromagnetic minerals from the high density fraction with a hand magnet and handpicked the remaining material for allanite. We selected allanite grains for large size, physical integrity, and the presence of glass adhering to the edges of the crystals. Fig. 1 shows a representative grain, which is approximately  $450 \times 275\ \mu\text{m}$ . Because allanite is almost opaque, it is not possible to avoid inclusion-bearing crystals, but the large

**Table 1**  
(U–Th)/He data and calculated helium eruption ages. The  $^{232}\text{Th}/^{230}\text{Th}$  shown is the average of  $n=4$  grains selected from the main population for thorium isotopic analysis. The 2 $\sigma$  standard deviation of the four samples was 3%.

Grain	Calculated mass mg	U ppm	Th ppm	$^{232}\text{Th}/^{230}\text{Th}$ Subpopulation average	He $10^{-10}$ moles/g	FT ( $\alpha$ -ejection correction)	Helium age ka	Helium age error (ka)
1	0.056	46	6600	323000	5.06	0.89	39.8	1.2
2	0.153	42	6600	323000	5.23	0.93	39.2	1.2
3	0.092	43	7700	323000	5.35	0.91	35.2	1.1
4	0.058	32	5700	323000	6.49	0.90		
5	0.062	48	7700	323000	5.66	0.90	37.7	1.1
6	0.101	39	7400	323000	5.78	0.91	39.5	1.2
7	0.099	65	12000	323000	8.02	0.91	34.9	1.1
8	0.043	25	4900	323000	3.80	0.89	40.3	1.2
9	0.057	52	9900	323000	7.10	0.90	36.9	1.1
10	0.061	45	7500	323000	6.20	0.90	41.8	1.3
11	0.050	43	7800	323000	5.49	0.89	36.6	1.1
12	0.043	60	9600	323000	8.09	0.88	43.5	1.3
13	0.039	39	6700	323000	5.27	0.88	40.8	1.2
14	0.043	42	7400	323000	5.67	0.89	39.7	1.2
15	0.075	25	4800	323000	3.47	0.90	37.2	1.1
16	0.041	44	6800	323000	4.94	0.88	37.7	1.1
17	0.060	33	5700	323000	4.30	0.90	38.8	1.2
Average							38.7	
SE (2 $\sigma$ )							1.2	

amounts of U and Th present in the allanite suggest that He ingrowth in inclusions is unimportant.

The selected allanite grains are predominantly anhedral to subhedral. Grains are also quite fragile: pressure applied with picking forceps causes grains to shatter and/or spall off adhering glass. From these observations we infer a high degree of physical preservation of the original crystal form for the grains we selected for analysis.

We analyzed a small number of grains using the American Museum of Natural History ESEM–EDX facility to ensure accurate identification of allanite. One of the eight studied grains, which in hindsight had an unusually elongate morphology, was amphibole. The seven remaining grains shared a highly unusual qualitative chemical composition, rich in Y, Th, and REE and characteristic of allanite (supplementary Fig. 2). The presence of the thorium peak was encouraging, as the detection limit for this technique is on the order of 1000 ppm.

### 3.2. (U–Th)/He analysis

We chose grains for (U–Th)/He analysis from the set of allanites analyzed by EDX and from similar grains from the same mineral

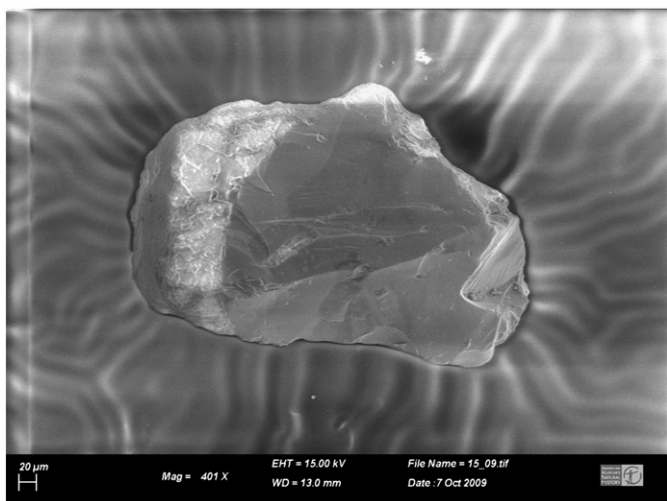


**Fig. 1.** SEM image of a representative allanite grain from this study showing characteristic volcanic glass adhered to the anhedral crystal.

separate. We encapsulated grains in HF-leached platinum tubes and then laser degassed them for  $^4\text{He}$  measurement by isotope dilution (House et al., 2000). After degassing we removed samples from the tubes into Teflon microvials, where we dissolved them in concentrated 2:1 HF:HNO<sub>3</sub>, dried them, and then brought them up in HNO<sub>3</sub>. An accurately measured small aliquot of each solution was taken from each sample, diluted due to the large thorium concentrations, and then measured for thorium and uranium by isotope dilution on a quadrupole ICP–MS with a collision cell to remove PtAr isobars in the U and Th mass spectrum. The analytical precision on these techniques yields formal (U–Th)/He age uncertainties of <2%.

Thorium isotope ratios were measured on a separate aliquot of several solutions using routine multicollector ICP–MS methods (e.g., Robinson et al., 2005). Procedural blanks were 300–600 pmol/g for U and 200–2500 pmol/g for Th. The analytical precision for each analysis was <0.5% and the standard deviation of the population thorium isotope ratio was 3%.

(U–Th)/He age determinations are typically made assuming that the uranium series daughters are in secular equilibrium. For samples that have undergone recent chemical fractionation (like Ash 15) this assumption is not likely to be valid. In such samples it is necessary to consider disequilibrium of  $^{230}\text{Th}$  in the radium series ( $^{238}\text{U}$ – $^{206}\text{Pb}$ ) decay chain (Farley et al., 2002). Given the very high Th/U in allanite we expect it to crystallize with a large  $^{230}\text{Th}$  excess. Indeed the dated allanites had Th/U ratios of up to  $\sim 200$  compared to  $3.05 \pm 0.082$  (1 $\sigma$ ) for shards of glass in the ash that we assume represent the magmatic source of the allanite. Such strong chemical fractionation of uranium from thorium implies a large excess (>50 fold) in the initial  $^{230}\text{Th}/^{238}\text{U}$  activity ratio.  $^{226}\text{Ra}$  ( $t_{1/2}=1,601$  a) disequilibrium may also occur, but its effect on the age is likely to be small due to the short half-life of this isotope. The actinium series ( $^{235}\text{U}$ – $^{207}\text{Pb}$ ) decay chain has one intermediate daughter with a significant lifetime ( $^{231}\text{Pa}$ ,  $t_{1/2}=32,760$  a). Because  $^{235}\text{U}$  is  $\sim 138$  times less abundant than  $^{238}\text{U}$ , we expect the effect of this disequilibrium to be much less important than  $^{230}\text{Th}$ . The thorium series ( $^{232}\text{Th}$ – $^{208}\text{Pb}$ ) decay chain has no long-lived intermediate daughters. Radium and protactinium disequilibria are unlikely to affect the reported ages outside of error and so we ignore them here. The contribution of  $^{147}\text{Sm}$  is also ignored—allanite typically contains about 3000 ppm Sm (e.g., Chesner and Ettlinger, 1989; Mcfarlane and McCulloch, 2007), an amount which would contribute  $\sim 0.2\%$  extra helium to crystals with actinide concentrations as high as those in the Ash 15 allanites.

Accounting for excess  $^{230}\text{Th}$  separately results in the following in-growth equation:

$${}^4\text{He} = 8 \cdot {}^{238}\text{U} (e^{\lambda_{238}t} - 1) + 7 \cdot \frac{{}^{238}\text{U}}{137.88} (e^{\lambda_{235}t} - 1) + 6 \cdot {}^{232}\text{Th} \left[ \frac{{}^{230}\text{Th} - {}^{230}\text{Th}_{\text{supp}}}{{}^{232}\text{Th}} (e^{\lambda_{230}t} - 1) + (e^{\lambda_{230}t} - 1) \right] \quad (1)$$

where  ${}^4\text{He}$ ,  ${}^{238}\text{U}$ ,  ${}^{232}\text{Th}$ , and  ${}^{230}\text{Th}$  are the current number of atoms of each isotope,  ${}^{230}\text{Th}_{\text{supp}}$  is the supported  ${}^{230}\text{Th}$  assuming secular equilibrium with  ${}^{238}\text{U}$ ,  $\lambda_i$  is the decay constant of isotope  $i$  in decays per year, and  $t$  is time in years.

To solve this equation we measured  ${}^{230}\text{Th}/{}^{232}\text{Th}$  directly on five allanite grains and use the population  ${}^{230}\text{Th}/{}^{232}\text{Th}$  ratio to calculate a  ${}^{230}\text{Th}$  concentration for each grain based on the single-grain  ${}^{232}\text{Th}$  measurements. The  ${}^{230}\text{Th}$  excess was calculated by subtracting  ${}^{230}\text{Th}$  supported by the decay of  ${}^{238}\text{U}$  from the following equation:

$${}^{230}\text{Th}_{\text{supp}} = \frac{\lambda_{238}}{\lambda_{230}} {}^{238}\text{U} \quad (2)$$

The choice of using the population average or single grain isotope ratio for each of the five grains analyzed for  ${}^{230}\text{Th}$  does not affect their ages within  $1\sigma$  analytical error. These measurements also allowed us to calculate  ${}^{230}\text{Th}$  excess disequilibrium ages for each of the five grains selected for  ${}^{230}\text{Th}$  analysis.

As with all (U-Th)/He measurements on small grains, a correction must be applied for the ejection of energetic alpha particles from the crystal (Farley et al., 1996), but this correction is small and imparts only minor uncertainty for crystals as large as the allanite grains in this study. As described above, we believe that the anhedral allanite grains we analyzed were not broken during sampling. Our reasoning does not exclude the possibility that grains were euhedral in the magma chamber and attained their current form during a violent eruption. However, potential abrasion during the eruptive event at zero helium retention is irrelevant for the alpha ejection correction.

Alpha ejection corrections were calculated according to the technique proposed by Farley et al. (1996) using Eq. (3).

$$F_T = 1 - \frac{S}{4} \cdot \frac{A}{V} \quad (3)$$

where  $F_T$  is the fraction of the total helium retained,  $S$  is the average stopping distance of the alpha particles in allanite,  $A$  is the surface area of the crystal, and  $V$  is the volume of the crystal. Surface area and volume were calculated as though the crystals are scalene ellipsoids, using the following equations.

$$V = \frac{4}{3} \pi \cdot a \cdot b \cdot c \quad (4)$$

where  $a$ ,  $b$ , and  $c$  are the three orthogonal axes measured for each crystal using an optical microscope. For surface area,

$$A = 4 \cdot \pi \cdot \left[ \frac{a^p b^p + a^p c^p + b^p c^p}{3} \right]^{1/2} \quad (5)$$

where  $p = 1.6075$  (Michon, 2011). This approximation is perfectly accurate for a sphere and is always accurate to within 1.061%. Errors in measurement and the geometric model are likely larger than errors associated with this mathematical approximation.

The value of  $S = 20.1 \mu\text{m}$  (the average stopping distance of alpha particles in allanite) was obtained using SRIM (Ziegler et al., 1985) with the alpha particle energy set to the average of alpha particles in the thorium series and radium series beginning with  ${}^{230}\text{Th}$ , the composition of the crystal defined as the IMA endmember allanite-(La), and the density set to  $3.93 \text{ g/cm}^3$  (Orlandi and Pasero, 2006).

While Ash 15 allanite is actually allanite-(Ce), with a La/Ce ratio slightly less than one (Supplementary Fig. 2), the REE composition of allanite-(La) more closely matches that of Ash 15 allanite than other reported endmembers. The density chosen is high within the range reported for allanite, and slight variations in composition and density do not change the calculated helium ages outside analytical error.

Results of the  $\alpha$  ejection computations are shown in Table 1. Almost all grains have  $F_T$  values of  $\sim 0.9$ , i.e., only about 10% of the alpha particles have been ejected.

### 3.3. ${}^{230}\text{Th}$ ages of Ash 15 allanite

We measured five specimens of glass to obtain an initial Th/U ratio of the allanite host magma of  $3.05 \pm 0.082$  ( $1\sigma$  SD), which we assume to be in secular equilibrium, as observed in glasses in the Mono Craters (Pickett and Murrell, 1997; Taddeucci et al., 1968). This allowed us to use the  ${}^{230}\text{Th}$  excess for each allanite analyzed for thorium isotopes to calculate a disequilibrium age according to the following set of equations.

First, Eq. (2) is used to calculate the amount of  ${}^{230}\text{Th}$  supported by  ${}^{238}\text{U}$  at secular equilibrium. This value, along with the  ${}^{230}\text{Th}$  concentration derived as described in Eq. (1), is used to calculate the “excess”  ${}^{230}\text{Th}$ :

$${}^{230}\text{Th}_{\text{excess}} = {}^{230}\text{Th} - {}^{230}\text{Th}_{\text{supp}} \quad (6)$$

After this calculation, the age is calculated using a standard age equation (Eq. (8)) for  ${}^{238}\text{U}$ - ${}^{230}\text{Th}$  disequilibrium, with the initial  ${}^{230}\text{Th}$  excess calculated according to Eq. (7). Eq. (7) assumes that  ${}^{232}\text{Th}$  and  ${}^{230}\text{Th}$  are fractionated into the allanite to the same degree relative to  ${}^{238}\text{U}$ , and makes use of the fact that the Th/U ratio is effectively constant over the time period of interest due to the very high  ${}^{232}\text{Th}/{}^{230}\text{Th}$  ratio and long half life of  ${}^{232}\text{Th}$ .

$${}^{230}\text{Th}_{\text{excess}}^{\text{initial}} = \frac{\text{Th}_{\text{allanite}}}{\text{Th}_{\text{glass}}} \cdot {}^{230}\text{Th}_{\text{supp}} \quad (7)$$

$$\text{Age} = \frac{-1}{\lambda_{230}} \ln \left[ \frac{{}^{230}\text{Th}_{\text{excess}}}{{}^{230}\text{Th}_{\text{excess}}^{\text{initial}}} \right] \quad (8)$$

We report individual disequilibrium age errors of 10%, which exceeds analytical precisions of  $<2\%$  on U and Th and  $\sim 3\%$  on  ${}^{232}\text{Th}/{}^{230}\text{Th}$  and reflects the distribution and small size of the age population. The difference between the  ${}^{230}\text{Th}$  crystallization age and the (U-Th)/He eruption age is the magma residence time of the crystal.

## 4. Results

### 4.1. Ash 15 eruption age

We analyzed 18 allanite grains for (U-Th)/He and five of these for  ${}^{230}\text{Th}$ . The (U-Th)/He analyses yielded a mean age of  $38.7 \pm 1.2 \text{ ka}$  (2 SE). (U-Th)/He data are summarized in Table 1. The  ${}^{230}\text{Th}$  contribution is not a correction – it is the actual contribution of the parent obtained by measuring  ${}^{232}\text{Th}/{}^{230}\text{Th}$  ratios for a subset of the allanite – so it is included in the calculated ages. The reported age is the apparent age after correction for alpha ejection.

Of the twenty grains selected for dating, one shattered after helium analysis, two gave no helium signal and were likely amphibole rather than allanite, and one (grain 4) gave an anomalously old helium age ( $3.5\sigma$  outlier). Relative to its calculated mass (by visual measurement of grain dimensions) and its measured mass (by microbalance), which are in good agreement, the anomalously old grain produced a typical concentration of helium but low uranium and

**Table 2**  
 $^{230}\text{Th}$  excess data and calculated disequilibrium crystallization ages.

Grain	$^{230}\text{Th}/^{238}\text{U}$	$^{230}\text{Th}/^{238}\text{U}$	$^{232}\text{Th}/^{238}\text{U}$	$^{232}\text{Th}/^{238}\text{U}$	Diseq. Age	
	Activity ratio	Activity ratio error	Activity ratio	Activity ratio error	ka	Error (ka)
1	38	0.11	65	0.10	65.7	6.6
8	35	0.14	61	0.14	68.0	6.8
11	34	0.094	59	0.083	66.3	6.6
13	34	0.13	58	0.11	64.0	6.4
					Average	66.0
					SD ( $2\sigma$ )	3.3

thorium, so we suspect that part of this grain was lost during transfer between the helium and the uranium–thorium analyses, probably during removal from the platinum tube. We removed this age from population calculations; inclusion increases the central tendency of the age population by just over 1000 years and more than doubles the standard deviation.

#### 4.2. Allanite magma residence time

Four grains measured for  $^{230}\text{Th}$  excess had Th/U ratios ranging from 144 to 193 and a population average  $^{232}\text{Th}/^{230}\text{Th}$  ratio of  $323000 \pm 10000$  ( $2\sigma$  SD). The calculated  $^{230}\text{Th}$  excess ages form a population with an age of  $66.0 \pm 3.3$  ka ( $2\sigma$  SD). Disequilibrium data are summarized in Table 2. One grain gave an anomalous Th/U ratio and anomalous Th and U concentrations during thorium isotope analysis, suggesting an error in sample dissolution or dilution, so we discard this result even though the thorium isotope ratio was consistent with the other grains. The calculated supported  $^{230}\text{Th}$  for each grain is two orders of magnitude lower than the initial  $^{230}\text{Th}$  excess. The  $^{230}\text{Th}$  excess in each crystal has declined by between 45% and 47% relative to the initial value we predict from the long-lived Th and U

isotopes in the coexisting glass, indicating excellent agreement among replicates and decay for approximately one half-life of  $^{230}\text{Th}$ .

A fortuitous byproduct of the need to measure  $^{230}\text{Th}$  is that we can calculate the residence time in the magma for the allanite crystals. To make this calculation, we assume that, while helium behaves as an open system in the magma chamber, the uranium–thorium system is closed in allanite after crystallization. Other researchers have argued that this is a reasonable assumption for other minerals (e.g., Reid et al., 1997; Scheibner et al., 2008) based on diffusion measurements of U and Th that demonstrate geologically insignificant diffusion rates in silicate minerals (Cherniak, 2010; Cherniak et al., 1997), and Vazquez and Reid (2004) demonstrated that allanite in a rhyolitic magma retains U and Th and that the  $^{238}\text{U}$ – $^{230}\text{Th}$  system records crystallization within the magma chamber. While U and Th transport may occur in highly radiation-damaged crystals (Geisler et al., 2002), this is only a concern for samples much older than the allanite in this study. The difference between the disequilibrium age and the (U–Th)/He age suggests a magmatic crystal residence time of about 30 ka for Ash 15 allanite (Fig. 2), which is consistent with short residence times observed for this phase in rhyolitic domes of the nearby Coso volcanic field (Simon et al., 2009).

The fact that the disequilibrium age is older than the (U–Th)/He age underscores that they record different phenomena: the disequilibrium age corresponds with the time elapsed since the crystal grew in the magma chamber, while the (U–Th)/He age indicates elapsed time since He accumulation began, i.e., upon eruption and cooling.

#### 5. Discussion and conclusions

The (U–Th)/He depositional age of  $38.7 \pm 1.2$  ka obtained on Ash 15 allanite provides a good constraint on the age of the geomagnetic excursion bisected by the ash. Our result is consistent with both the Zimmerman et al. (2006) age model that pins Ash 15 at 39.8 ka, and

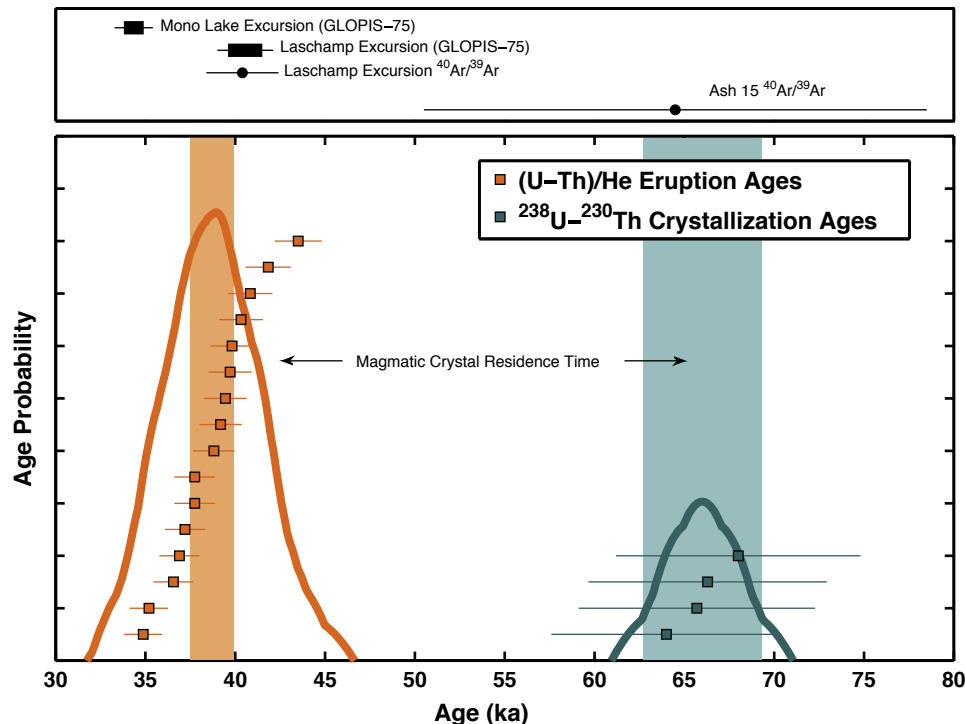


**Fig. 2.** (U–Th)/He eruption ages and  $^{238}\text{U}$ – $^{230}\text{Th}$  crystallization ages for the allanite grains from Wilson Creek Formation Ash 15. The global paleomagnetic record dates for the Mono Lake Excursion and the Laschamp Excursion (GLOPIS–75; Laj et al., 2004) and the volcanic  $^{40}\text{Ar}/^{39}\text{Ar}$  sanidine date for the Laschamp Excursion (40.4 ka; Guillou et al., 2004) are shown along with the mean age of sanidine from Ash 15 (Kent et al., 2002) and the ~30 ka magmatic crystal residence time implied by the (U–Th)/He and  $^{238}\text{U}$ – $^{230}\text{Th}$  ages. The lightly shaded boxes represent the mean age and reported error for each age population.

with the age of the Laschamp at its type locality,  $40.4 \pm 2$  ka (Guillou et al., 2004). Ash 15 is located about 20 cm ( $\sim 1$  ka) above the paleointensity minimum (Zimmerman et al., 2006), so the implied age of the excursion is even closer to the Laschamp type locality than the Ash 15 allanite age. With the addition of this new age constraint the Mono Lake Excursion at its type locality shares a similar structure, timescale, and age with the Laschamp. Since only one excursion is recorded in the Wilson Creek Formation, it seems most parsimonious to conclude that the Ash 15 excursion is indeed a record of the Laschamp. Ironically, the so-called Mono Lake Event observed in marine records (Laj et al., 2004) is apparently either absent or only weakly expressed in Mono Lake sediments.

Alternative techniques have yielded unreliable ages due to difficulties with the radiocarbon system and a dispersed and apparently unreasonable old  $^{40}\text{Ar}/^{39}\text{Ar}$  sanidine population (Cassata et al., 2010; Kent et al., 2002; Zimmerman et al., 2006). While the challenges of radiocarbon dating in exotic and contaminated systems near the upper age limit of the radiocarbon system are well recognized (e.g., Pigati et al., 2007), the failure of the  $^{40}\text{Ar}/^{39}\text{Ar}$  sanidine method is more difficult to explain. The problem in the case of WCF Ash 15 is apparently either “excess argon,” a poorly understood phenomenon, or simply inheritance of older sanidine from the country rock. While we emphasize that it may be a coincidence, the central tendency of our  $^{230}\text{Th}$  excess ages,  $66.0 \pm 3.3$  ka, overlaps with that of the  $^{40}\text{Ar}/^{39}\text{Ar}$  sanidine population,  $64.5 \pm 13$  ka (Kent et al., 2002). If sanidine crystallized around the same time as allanite, the  $^{40}\text{Ar}/^{39}\text{Ar}$  sanidine ages may represent retention of argon in sanidine in the magma chamber. This finding potentially supports recent evidence of argon retention in minerals in a magma chamber by Hora et al. (2010), although in a mineral that these authors found to be devoid of pre-eruptive argon. This discrepancy may indicate different pre-eruptive P–T conditions in this magmatic system, a difference in magmatic argon pressure, or simply the greater sensitivity of the (U–Th)/He system to detecting excess argon in sanidine.

The calculated  $^{230}\text{Th}$  excess ages form a population with an age of  $66.0 \pm 3.3$  ka ( $2\sigma$  SD). Given the eruption age of  $38.7 \pm 1.2$  ka, this suggests a magma residence time for these allanites of slightly less than 30 ka. In addition to the small sample size, we note that the apparent frequency of eruptions in this system may restrict the distribution of crystallization ages in a given ash. The ability to calculate a crystal residence time on the basis of a (U–Th)/He age and a  $^{238}\text{Th}$ – $^{230}\text{Th}$  crystallization age for the same mineral complements other methods that provide a measure of crystal residence times (Brown and Fletcher, 1999; Miller and Wooden, 2004; Reid and Coath, 2000; Reid et al., 1997; Simon et al., 2008). Combining (U–Th)/He dating and  $^{238}\text{U}$ – $^{230}\text{Th}$  disequilibrium dating on single crystals of the same mineral is especially valuable for crystal residence time calculations in young magmatic systems for which U–Pb dating is not feasible but in which other methods are most likely to achieve the sensitivity necessary to detect residence times of less than 100 kyr.

## Acknowledgments

We thank Gary Hemming and Guleed Ali for help with sampling and logistics, Lindsey Hedges and Adam Subhas for help with chemistry and analysis, and Becky Rudolph for assistance with the SEM. This research was supported by the Columbia Climate Center and the Comer Foundation, and by the National Science Foundation through a Graduate Research Fellowship to S. E. Cox.

## Appendix A. Supplementary data

Supplementary data to this article can be found online at doi:10.1016/j.epsl.2011.12.025.

## References

- Aciego, S., Kennedy, B., DePaolo, D., Christensen, J., Hutcheon, I., 2003. U–Th/He age of phenocrystic garnet from the 79 AD eruption of Mt. Vesuvius. *Earth Planet. Sci. Lett.* 219, 209–219.
- Benson, L., Burdett, J., Lund, S., Kashgarian, M., 1997. Nearly synchronous climate change in the Northern Hemisphere during the last glacial termination. *Nature* 388, 263–265.
- Benson, L., Currey, D., Dorn, R., Lajoie, K., Oviatt, C., Robinson, S., Smith, G., Stine, S., 1990. Chronology of expansion and contraction of four great Basin lake systems during the past 35,000 years. *Palaeogeogr. Palaeoclimatol. Palaeoecol.* 78, 241–286.
- Benson, L., Liddicoat, J., Smoot, J., Sarna-Wojcicki, A., Negrini, R., Lund, S., 2003. Age of the Mono Lake excursion and associated tephra. *Quat. Sci. Rev.* 22, 135–140.
- Benson, L., Lund, S., Burdett, J., Kashgarian, M., Rose, T., Smoot, J., Schwartz, M., 1998. Correlation of late-Pleistocene lake-level oscillations in Mono Lake, California, with North Atlantic climate events. *Quat. Res.* 49, 1–10.
- Brown, S., Fletcher, I., 1999. SHRIMP U–Pb dating of the preeruption growth history of zircons from the 340 ka Whakamaru Ignimbrite, New Zealand: evidence for >250 kyr magma residence times. *Geology* 27, 1035–1038.
- Bursik, M., Gillespie, A., 1993. Late pleistocene glaciation of Mono Basin, California. *Quat. Res.* 39, 24–35.
- Cassata, W.S., Singer, B.S., Liddicoat, J.C., Coe, R.S., 2010. Reconciling discrepant chronologies for the geomagnetic excursion in the Mono Basin, California: Insights from new  $^{40}\text{Ar}/^{39}\text{Ar}$  dating experiments and a revised relative paleointensity correlation. *Quat. Geochronol.* 5, 533–543.
- Chen, Y., Smith, P., Evensen, N., York, D., Lajoie, K., 1996. The edge of time: dating young volcanic ash layers with the  $^{40}\text{Ar}$ – $^{39}\text{Ar}$  laser probe. *Science* 274, 1176–1178.
- Cherniak, D., 2010. Diffusion in accessory minerals: zircon, titanite, apatite, monazite, and xenotime. In: Zhang, Y., Cherniak, D.J. (Eds.), *Diffusion in Minerals and Melts: Reviews in Mineralogy and Geochemistry*, pp. 899–920.
- Cherniak, D., Hanchar, J., Watson, E., 1997. Diffusion of tetravalent cations in zircon. *Contrib. Mineral. Petrol.* 127, 383–390.
- Chesner, C., Ettliger, A., 1989. Composition of volcanic allanite from the Toba Tuffs, Sumatra, Indonesia. *Am. Mineral.* 74, 750–758.
- Coe, R., Singer, B., Pringle, M., 2004. Matuyama–Brunhes reversal and Kamikatsura event on Maui: paleomagnetic directions,  $^{40}\text{Ar}/^{39}\text{Ar}$  ages and implications. *Earth Planet. Sci. Lett.* 222, 667–684.
- Crowley, J.L., Schoene, B., Bowring, S.A., 2007. U–Pb dating of zircon in the Bishop Tuff at the millennial scale. *Geology* 35, 1123.
- Davidson, J., Hassanzadeh, J., Berzins, R., Stockli, D., Bashukoo, B., Turrin, B., Pandamouz, A., 2004. The geology of Damavand volcano, Alborz Mountains, northern Iran. *GSA Bull.* 116, 16–29.
- Davis, O., 1999. Pollen analysis of a late-glacial and Holocene sediment core from Mono Lake, Mono County, California. *Quat. Res.* 52, 243–249.
- Denham, C.R., Cox, A., 1971. Evidence that the Laschamp polarity event did not occur 13 300–30 400 years ago. *Earth Planet. Sci. Lett.* 13, 181–190.
- Farley, K., Kohn, B., Pillans, B., 2002. The effects of secular disequilibrium on (U–Th)/He systematics and dating of Quaternary volcanic zircon and apatite. *Earth Planet. Sci. Lett.* 201, 117–125.
- Farley, K., Wolf, R., Silver, L., 1996. The effects of long alpha-stopping distances on (U–Th)/He ages. *Geochim. Cosmochim. Acta* 60, 4223–4229.
- Geisler, T., Pidgeon, R., Van Bronswijk, W., Kurtz, R., 2002. Transport of uranium, thorium, and lead in metamict zircon under low-temperature hydrothermal conditions. *Chem. Geol.* 191, 141–154.
- Graham, N.E., Hughes, M.K., 2007. Reconstructing the Mediaeval low stands of Mono Lake, Sierra Nevada, California, USA. *Holocene* 17, 1197–1210.
- Guillou, H., Singer, B., Laj, C., Kissel, C., 2004. On the age of the Laschamp geomagnetic excursion. *Earth Planet. Sci. Lett.* 227, 331–343.
- Hora, J., Singer, B., Jicha, B., Beard, B., Johnson, C., de Silva, S., Salisbury, M., 2010. Volcanic biotite–sanidine  $^{40}\text{Ar}/^{39}\text{Ar}$  age discordances reflect Ar partitioning and pre-eruption closure in biotite. *Geology* 38, 923–926.
- House, M., Farley, K., Stockli, D., 2000. Helium chronometry of apatite and titanite using Nd–YAG laser heating. *Earth Planet. Sci. Lett.* 183, 365–368.
- Kent, D.V., Hemming, S.R., Turrin, B.D., 2002. Laschamp Excursion at Mono Lake? *Earth Planet. Sci. Lett.* 197, 151–164.
- Laj, C., Kissel, C., Beer, J., 2004. High resolution global paleointensity stack since 75 kyr (GLOPIS-75) calibrated to absolute values. In: Channell, J.E.T., Kent, D.V., Lowrie, W., Meert, J.G. (Eds.), *Timescales of the Paleomagnetic Field*. Geophysical Monograph. American Geophysical Union, Washington, DC, pp. 255–265.
- Lajoie, K., 1968. Late Quaternary stratigraphy and geologic history of Mono Basin, Eastern California. PhD Dissertation, University of California.
- Liddicoat, J., Coe, R., 1979. Mono Lake geomagnetic excursion. *J. Geophys. Res.* 84, 261–271.
- Lund, S.P., Liddicoat, J.C., Lajoie, K.R., Henyey, T.L., Robinson, S.W., 1988. Paleomagnetic evidence for long-term (104 year) memory and periodic behavior in the Earth's core dynamo process. *Geophys. Res. Lett.* 15, 1101–1104.
- McFarlane, C., McCulloch, M., 2007. Coupling of in-situ Sm–Nd systematics and U–Pb dating of monazite and allanite with applications to crustal evolution studies. *Chem. Geol.* 245, 45–60.
- Michon, G.P., 2011. Surface Area of an Ellipsoid. Retrieved 2011-08-19, 2011, from Numerica. <http://www.numerica.com/answer/ellipsoid.htm-thomsen> (06–06).
- Miller, J., Wooden, J., 2004. Residence, resorption and recycling of zircons in Devils Kitchen rhyolite, Coso volcanic field, California. *J. Petrol.* 45, 2155–2170.
- Orlandi, P., Pasero, M., 2006. Allanite-(La) from Buca della Vena mine, Apuan Alps, Italy, an epidote-group mineral. *Can. Mineral.* 44, 63–68.

- Pickett, D., Murrell, M., 1997. Observations of  $^{231}\text{Pa}/^{235}\text{U}$  disequilibrium in volcanic rock. *Earth Planet. Sci. Lett.* 148, 259–271.
- Pigati, J., Quade, J., Wilson, J., Jull, A., Lifton, N., 2007. Development of low-background vacuum extraction and graphitization systems for  $^{14}\text{C}$  dating of old (40–60 ka) samples. *Quat. Int.* 166, 4–14.
- Reheis, M., Stine, S., Sarna-Wojcicki, A., 2002. Drainage reversals in Mono Basin during the late Pliocene and Pleistocene. *GSA Bull.* 114, 991–1006.
- Reid, M.R., Coath, C., 2000. In situ U–Pb ages of zircons from the Bishop Tuff: no evidence for long crystal residence times. *Geology* 28, 443–446.
- Reid, M.R., Coath, C., Harrison, T., McKeegan, K., 1997. Prolonged residence times for the youngest rhyolites associated with Long Valley Caldera:  $^{230}\text{Th}$ – $^{238}\text{U}$  ion microprobe dating of young zircons. *Earth Planet. Sci. Lett.* 150, 27–39.
- Robinson, L., Adkins, J., Keigwin, L., Southon, J., 2005. Radiocarbon variability in the western North Atlantic during the last deglaciation. *Science* 310, 1469–1473.
- Russell, I., 1889. Quaternary history of Mono Valley, California. USGS Eighth Annual Report. Government Printing Office, Washington, pp. 261–394.
- Scheibner, B., Heumann, A., Wörner, G., Civetta, L., 2008. Crustal residence times of explosive phonolite magmas: U–Th ages of magmatic Ca-garnets of Mt. Somma-Vesuvius (Italy). *Earth Planet. Sci. Lett.* 276, 293–301.
- Schmitt, A., Grove, M., Harrison, T., Lovera, O., Hulen, J., Walters, M., 2003. The Geysers - Cobb Mountain Magma System, California (Part 1): U–Pb zircon ages of volcanic rocks, conditions of zircon crystallization and magma residence times. *Geochim. Cosmochim. Acta* 67, 3423–3442.
- Simon, J., Renne, P., Mundil, R., 2008. Implications of pre-eruptive magmatic histories of zircons for U–Pb geochronology of silicic extrusions. *Earth Planet. Sci. Lett.* 266, 182–194.
- Simon, J., Vazquez, J., Renne, P., Schmitt, A., Bacon, C., Reid, M., 2009. Accessory mineral U–Th–Pb ages and  $^{40}\text{Ar}/^{39}\text{Ar}$  eruption chronology, and their bearing on rhyolitic magma evolution in the Pleistocene Coso volcanic field, California. *Contrib. Mineral. Petrol.* 158, 421–446.
- Stine, S., 1987. Mono Lake; the past 4,000 years. PhD Dissertation, University of California, Berkeley.
- Stine, S., 1990a. Late Holocene fluctuations of Mono Lake, eastern California. *Palaeogeogr. Palaeoclimatol. Palaeoecol.* 78, 333–381.
- Stine, S., 1990b. Past climate at Mono Lake. *Nature* 345, 391.
- Taddeucci, A., Broecker, W., Thurber, D., 1968.  $^{230}\text{Th}$  dating of volcanic rocks. *Earth Planet. Sci. Lett.* 3, 338–342.
- Vazquez, J., Reid, M., 2004. Probing the accumulation history of the voluminous Toba magma. *Science* 305, 991–994.
- Wolf, R., 1997. The development of the (U–Th)/He thermochronometer. PhD Dissertation, California Institute of Technology.
- Ziegler, J., Biersack, J., Littmark, U., 1985. The stopping and range of ions in solids. Pergamon Press, New York.
- Zimmerman, S., Hemming, S.R., Kent, D., Searle, S., 2006. Revised chronology for late Pleistocene Mono Lake sediments based on paleointensity correlation to the global reference curve. *Earth Planet. Sci. Lett.* 252, 94–106.
- Zimmerman, S., Hemming, S.R., Hemming, N.G., Tomascak, P.B., Pearl, C., 2011a. High-resolution chemostratigraphic record of late Pleistocene lake-level variability, Mono Lake, CA. *GSA Bulletin* 123, 2320–2334.
- Zimmerman, S., Pearl, C., Hemming, S.R., Tamulonis, K., Hemming, N.G., Searle, S., 2011b. Freshwater control of ice-rafted debris in the last glacial period at Mono Lake, California, USA. *Quat. Res.* 76, 264–271.